

Figure S1

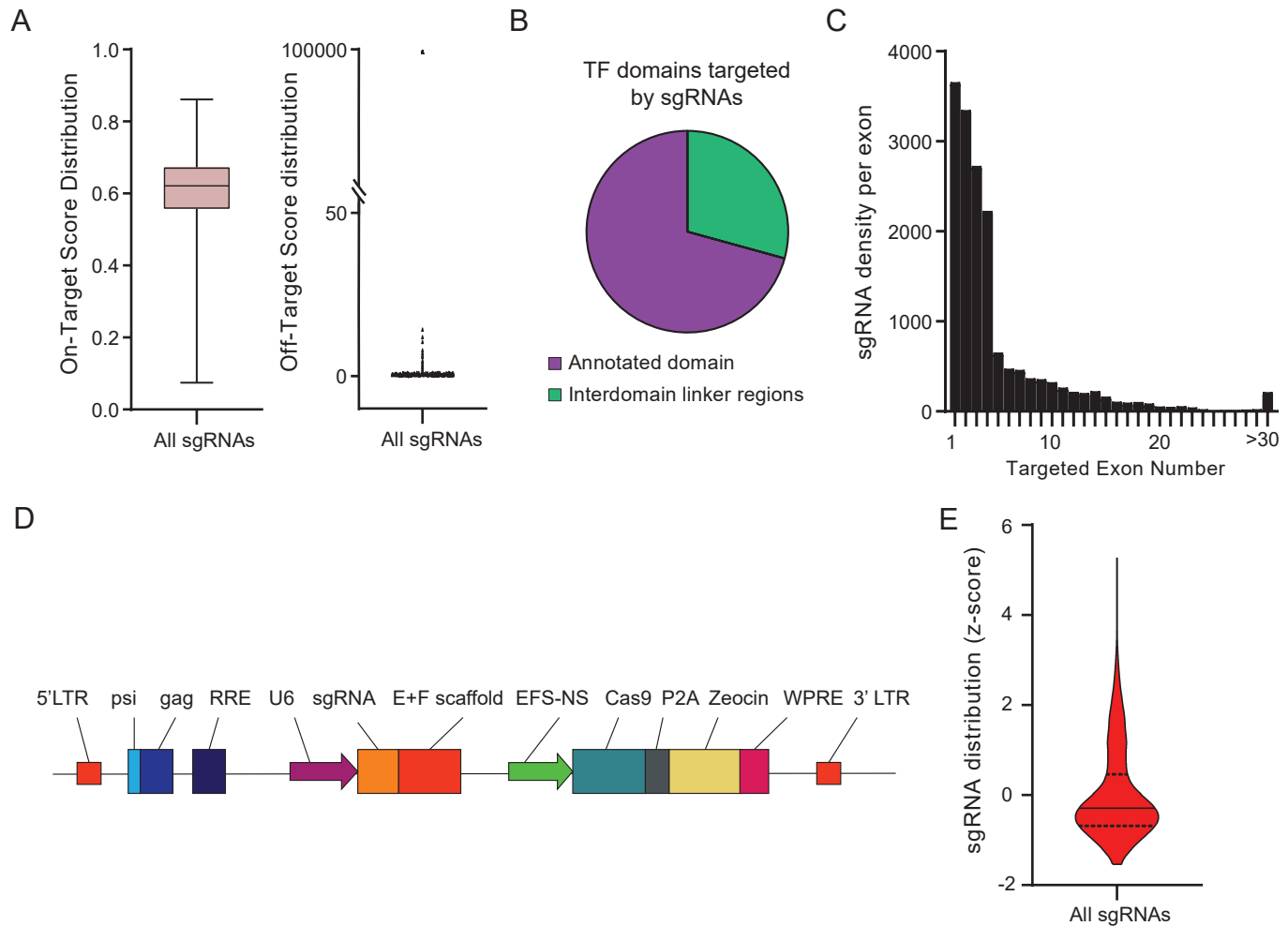
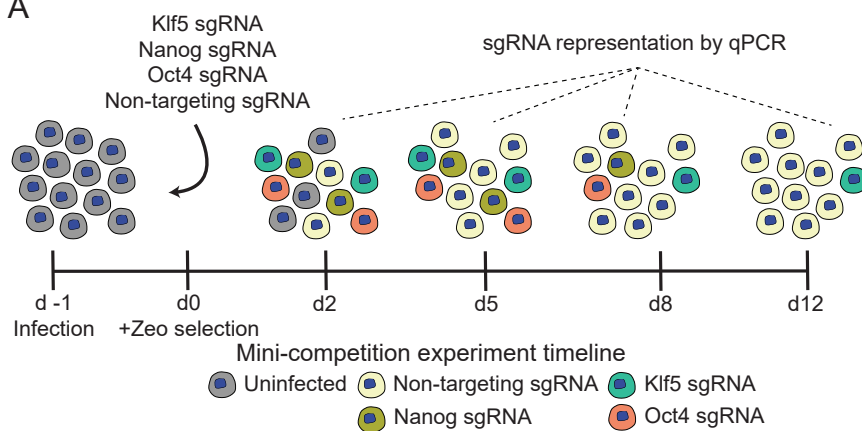


Figure S1. CRISPR TF library targets 1682 TFs in the mouse genome.

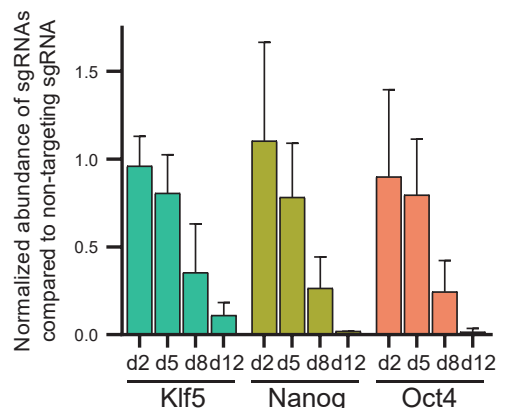
- (A)** On-target and off-target score distribution of all sgRNAs in the library based on the GUIDE algorithm.
- (B)** Percentage of targeted annotated TF domains in the library based on Pfam. 71% of the sgRNAs target an annotated functional domain.
- (C)** Exon targeting density of sgRNAs in the library. sgRNAs were designed to target 5' exons to increase the chance of generating a frameshift.
- (D)** The lentiviral expression vector for sgRNA and Cas9. psi+, Psi packaging signal; RRE, Rev response element; cPPT, central polypurine tract; EFS, elongation factor 1a short promoter; Flag, Flag octapeptide tag; P2A, 2A self-cleaving peptide; Zeo, zeocin resistance gene; WPRE, post-transcriptional regulatory element; EF1a, elongation factor 1a promoter.
- (E)** Representation of the normalized number of reads of sgRNAs in the plasmid library with Z-score distribution. The solid line represents the mean z-score. Dashed lines represent quartiles.

Figure S2

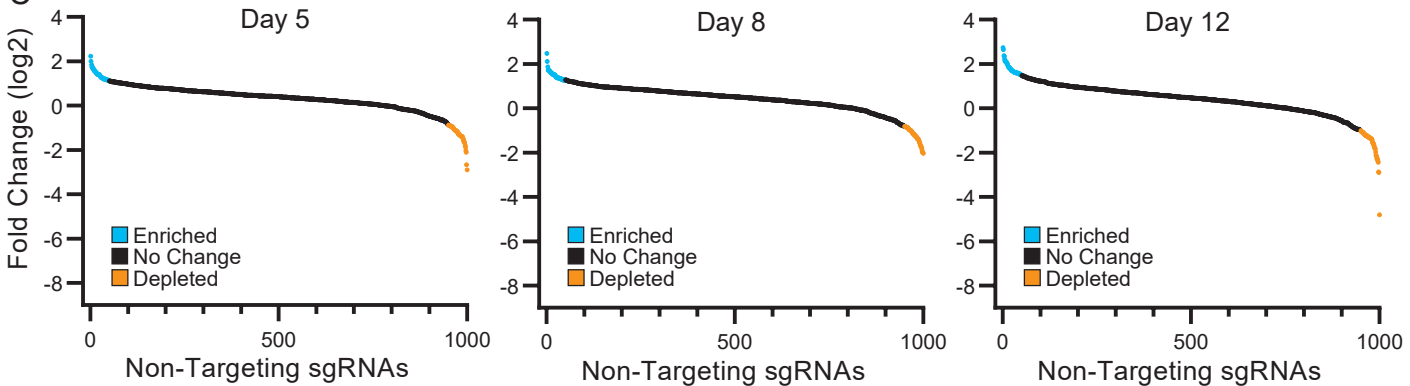
A



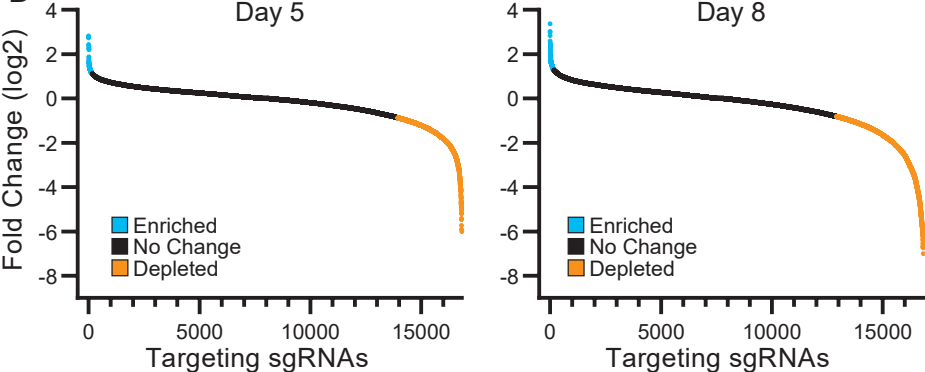
B



C



D



E

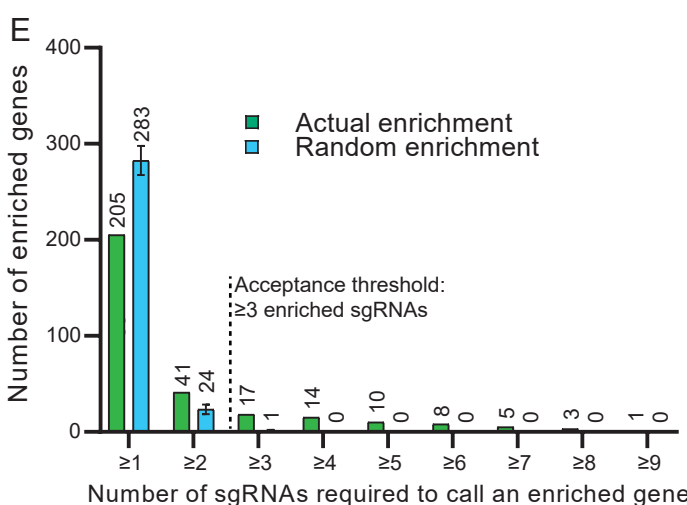


Figure S2. Determination of candidate factors based on the false discovery rate from non-targeting sgRNAs.

- (A)** Schematic overview of the qPCR competition assay to identify depletion dynamics. Representation of non-targeting and *Klf5*, *Oct4*, and *Nanog* targeting sgRNAs infected cells over 12 days of culture.
- (B)** Normalized abundance of *Klf5*, *Oct4*, *Nanog* targeting sgRNAs compared to non-targeting sgRNA with qPCR in collected samples for each time point (n=2). The abundance of pluripotency TFs is nullified within 12d.
- (C)** Log2 fold change of non-targeting sgRNAs on day 5, day 8, day 12 compared to the initial library representation. 50 most enriched sgRNAs are in blue and 50 most depleted sgRNAs are in orange. 50th most enriched and 50th most depleted sgRNAs were selected as the thresholds to call depleted and enriched targeting sgRNAs for each timepoint.
- (D)** Log2 fold change of targeting sgRNAs on day 5 and day 8 compared to the initial library representation. sgRNAs depleted more than the 50th most depleted non-targeting sgRNA are in orange and enriched more than the 50th most enriched non-targeting sgRNA are in blue.
- (E)** The number of actual sgRNAs enriched and mean sgRNAs number with random enrichment calculated by 1000 permutation tests with a different number of sgRNA per gene thresholds. TFs with more than or equal to 3 enriched sgRNAs are unlikely to be false positives.

Figure S3

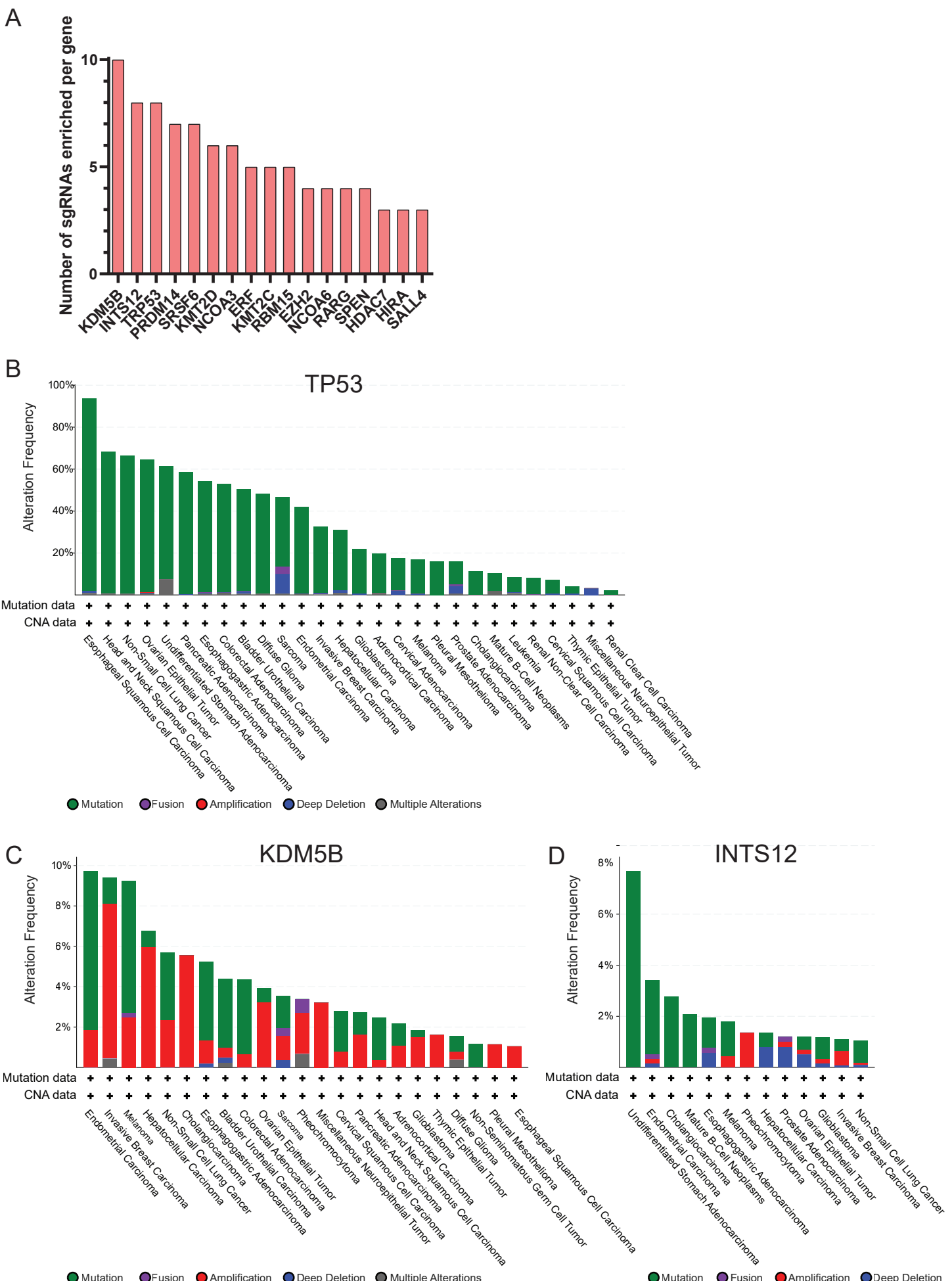


Figure S3. Enriched genes are mutated in cancers.

(A) 17 genes have 3 or more sgRNAs enriched on day 12.

(B) *Tp53*, **(C)** *Kdm2b*, **(D)** *Ints12* mutations incidence in various types of cancers (51799 patients). Data obtained from cBioPortal for Cancer Genomics. Enriched sgRNAs are targeting genes that are growth limiting, which are also found in cancer types.

Figure S4

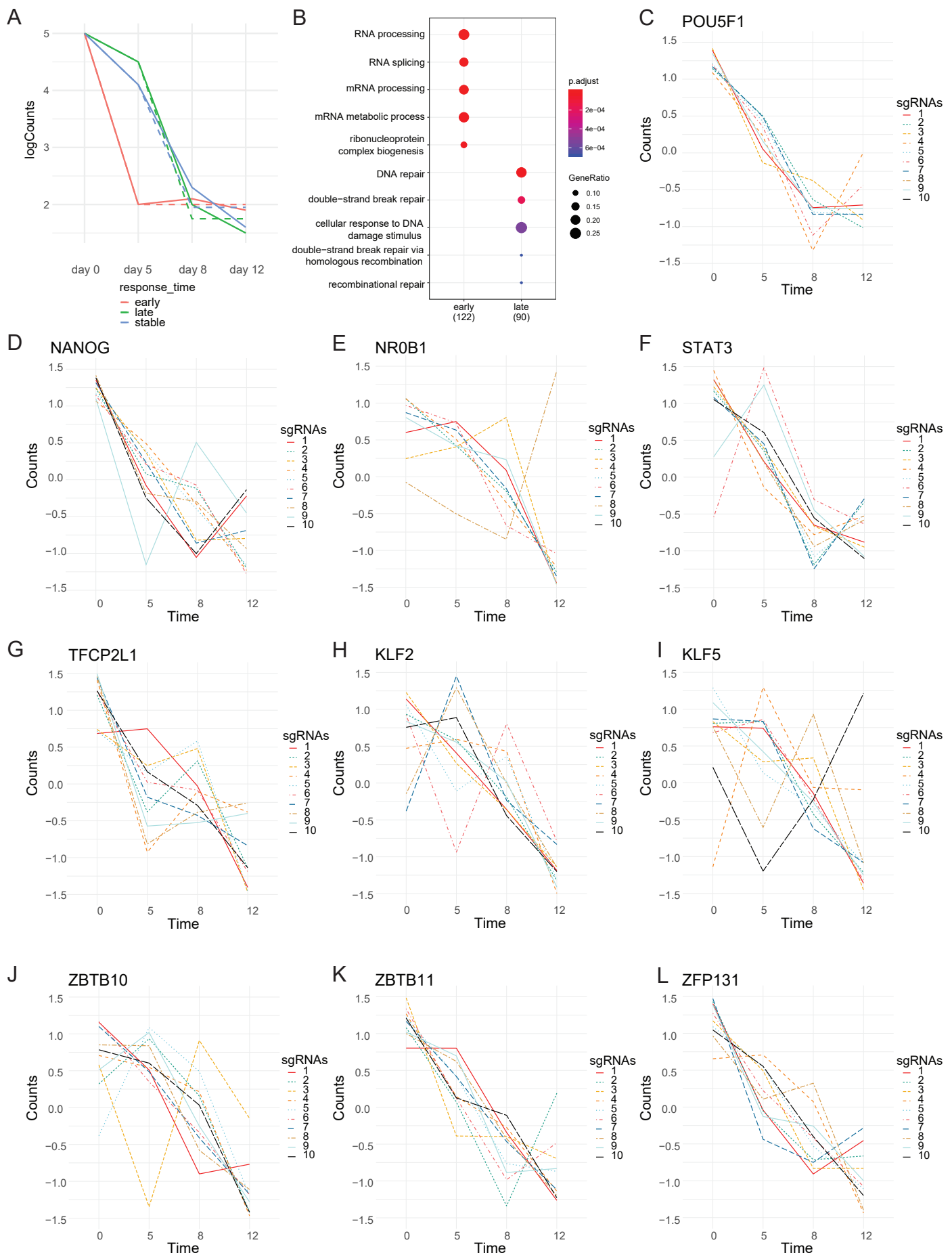


Figure S4. Determination of candidate factors using a linear modeling method.

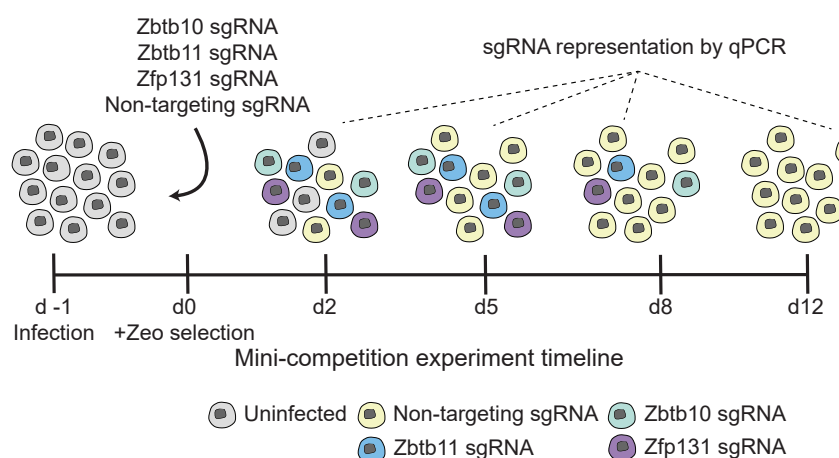
(A) Linear modeling for differential depletion categories of genes based on normalized sgRNA log counts. Three categories: early, stable, and late depleting were identified. The solid line is how the linear modeling is predicted and the dashed line is how the data fit to the projection.

(B) GO-enrichment analysis of early (n=122) and late (n=90) depleting factors throughout the screen. Gene Ratio is calculated with the number of occurrences in specific GO categories divided by the total amount of depleted TFs per category. Early category contains genes that are in core transcription machinery whereas late category contains genes that are playing roles in DNA damage.

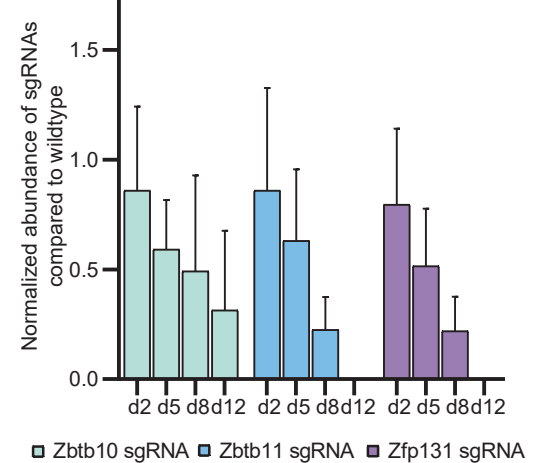
(C) Linear regression of 10 sgRNAs targeting known core pluripotency factors **(D)** *Oct4*, **(D)** *Nanog*, accessory factors **(E)** *Nr0b1*, **(F)** *Stat3*, **(G)** *Tfcp2l1*, redundant accessory factors **(H)** *Klf2*, **(I)** *Klf5* and candidate hits from the screen **(J)** *Zbtb10*, **(K)** *Zbtb11*, **(L)** *Zfp131*. *Oct4*, *Nanog*, *Zbtb11*, and *Zfp131* are in the early depleting category whereas accessory factors and *Zbtb10* are in the stable and the late depleting categories.

Figure S5

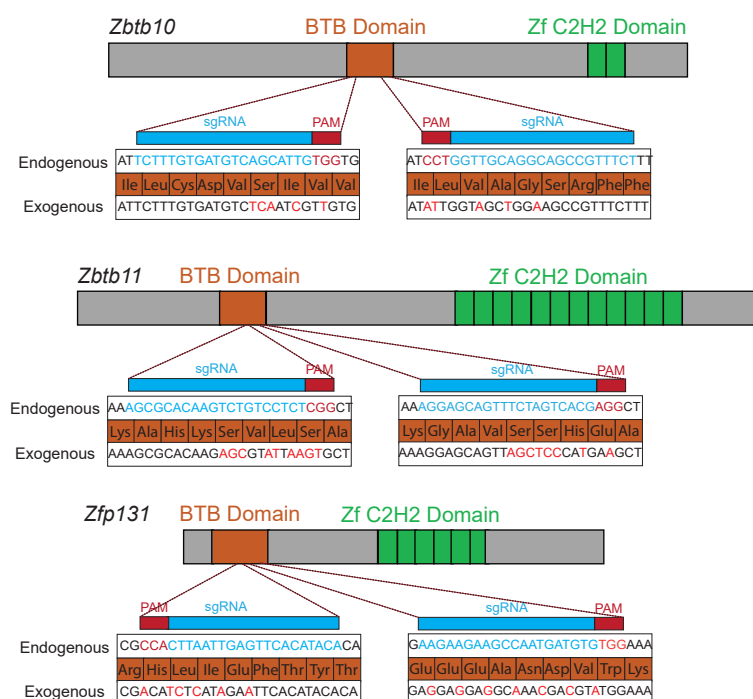
A



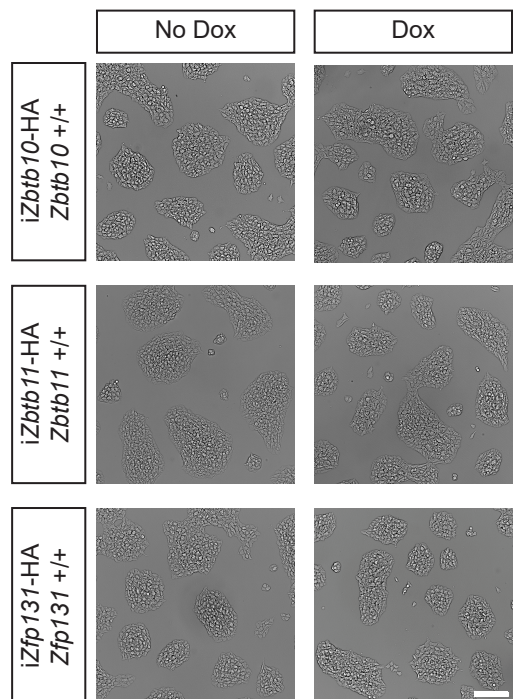
B



C



D



E

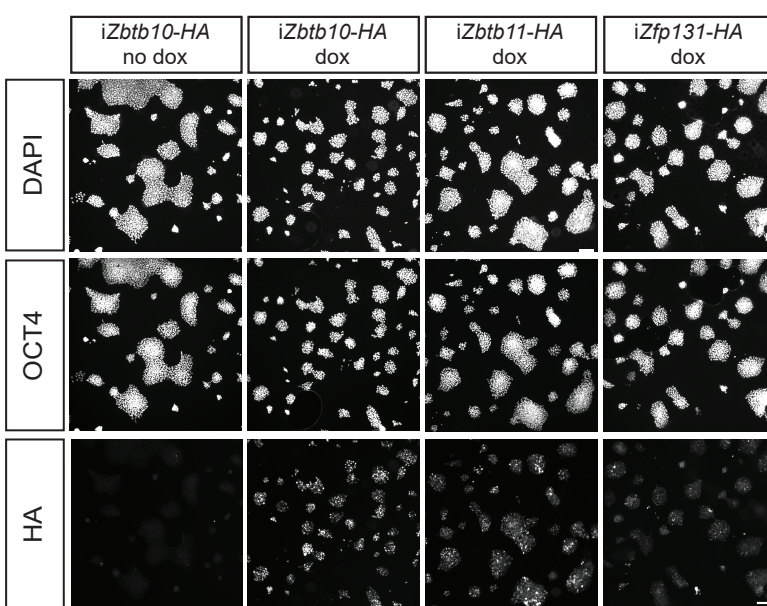
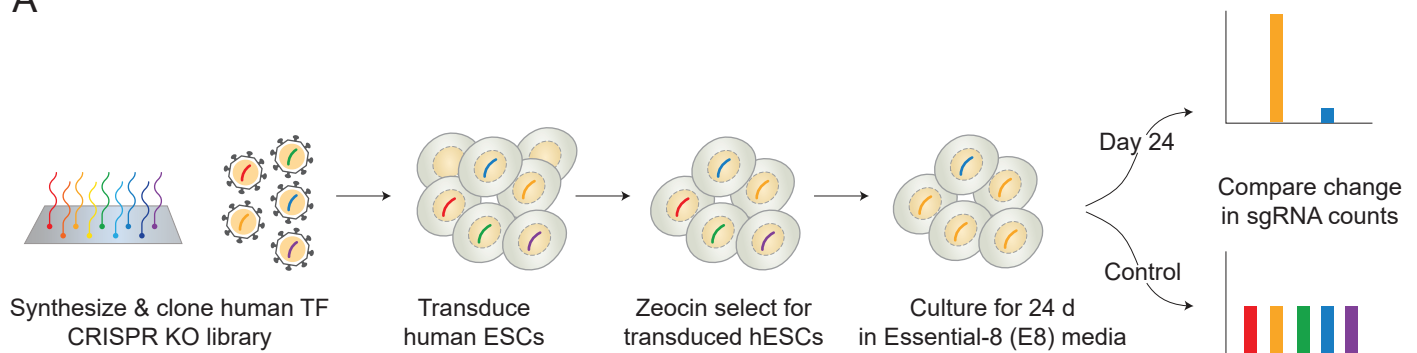


Figure S5. Generation of conditional *Zbtb10*Δ, *Zbtb11*Δ, and *Zfp131*Δ lines

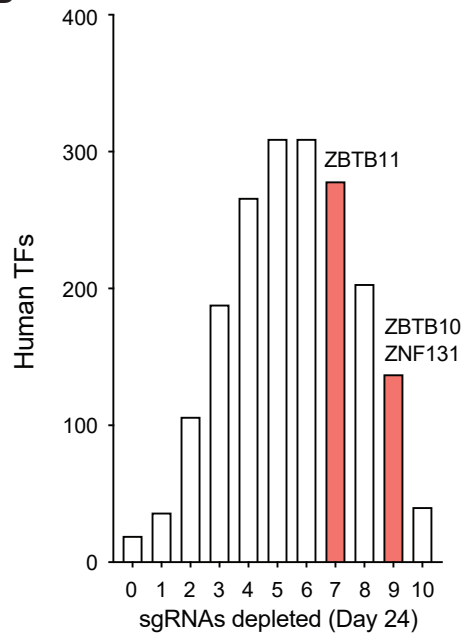
- (A)** Schematic overview of the TF candidate qPCR competition assay. Non-targeting and *Zbtb10*, *Zbtb11*, and *Zfp131* targeting sgRNAs infected cells representation over 12 days of culture.
- (B)** Normalized abundance of targeting sgRNAs compared to non-targeting sgRNA measured by qPCR in the competition experiment (n=2). *Zbtb10*, *Zbtb11*, and *Zfp131* targeting sgRNAs deplete compared to non-targeting one recapitulating the TF screen depletion dynamics.
- (C)** *Zbtb10*, *Zbtb11* and *Zfp131* genes illustrated with coding regions for interdomain linker regions (gray), BTB domain (orange) and C2H2 Zinc Finger domain (green). Two sgRNAs (blue sequences) targeting PAM sites (red sequences) at the endogenous BTB domain. HA-tagged exogenous copy of ZBTB10, ZBTB11, and ZFP131 expressed at the HPRT site contain silent mutations that disable the sgRNA binding and Cas9 cutting.
- (D)** Inducible *Zbtb10-HA*, *Zbtb11-HA* and *Zfp131-HA* lines with 48 h expression of exogenous alleles. Inducing transgenes do not cause any distinct morphological changes in ESCs. Scale bar = 200 μm.
- (E)** Oct4 and HA staining of inducible *Zbtb10-HA*, *Zbtb11-HA* and *Zfp131-HA* lines with 48h expression of exogenous alleles. Inducing transgenes do not alter *Oct4* expression in ESCs. Scale bar = 100 μm.

Figure S6

A



B



C

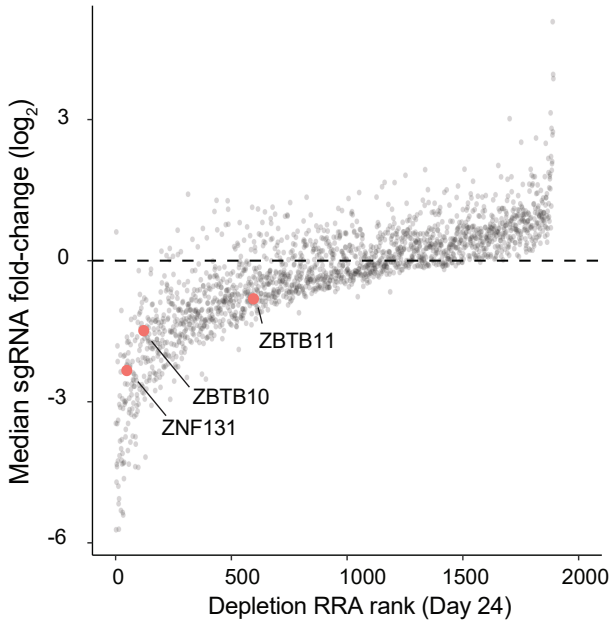


Figure S6. Human embryonic stem cell CRISPR screen identifies ZBTB10, ZBTB11 and ZNF131 as depleting genes.

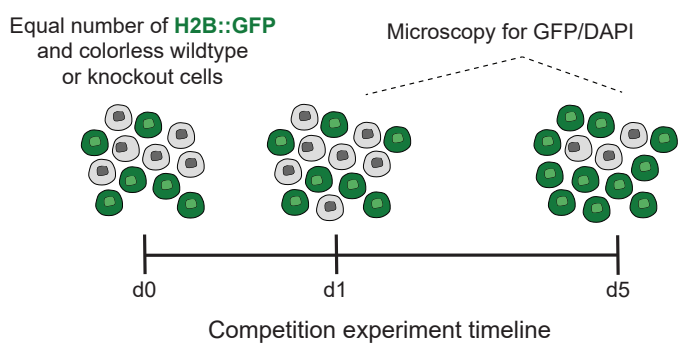
(A) Schematic of human embryonic stem cell screen for TFs.

(B) Number of depleted sgRNAs for each TF using FDR < 0.05 threshold, as calculated from the non-targeting sgRNAs. ZBTB11 has 7 depleted sgRNAs, whereas ZBTB10 and ZNF131 have 9 depleted sgRNAs in hESCs.

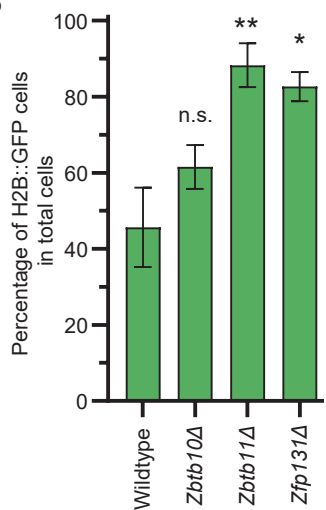
(C) Median sgRNAs fold-change (log2) at day 24 as a function of RRA gene rank. sgRNAs targeting ZBTB10, ZBTB11 and ZFP131 have lower median rank denoting their role in hESCs.

Figure S7

A



B



C

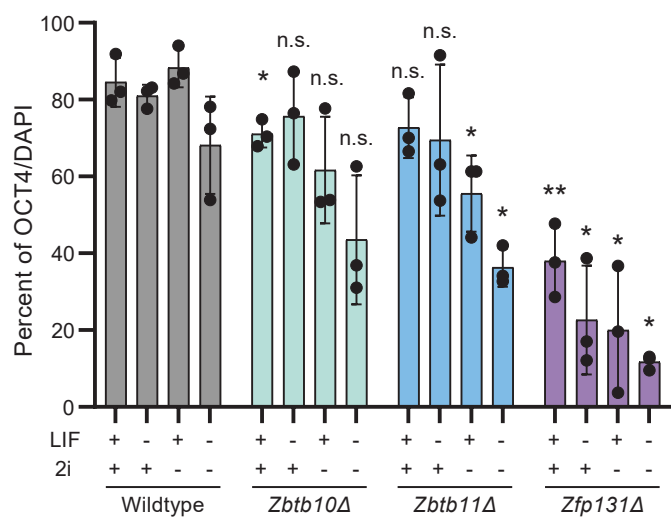


Figure S7. *Zbtb11* Δ and *Zfp131* Δ mutant cells have reduced proliferation and differentiation phenotypes.

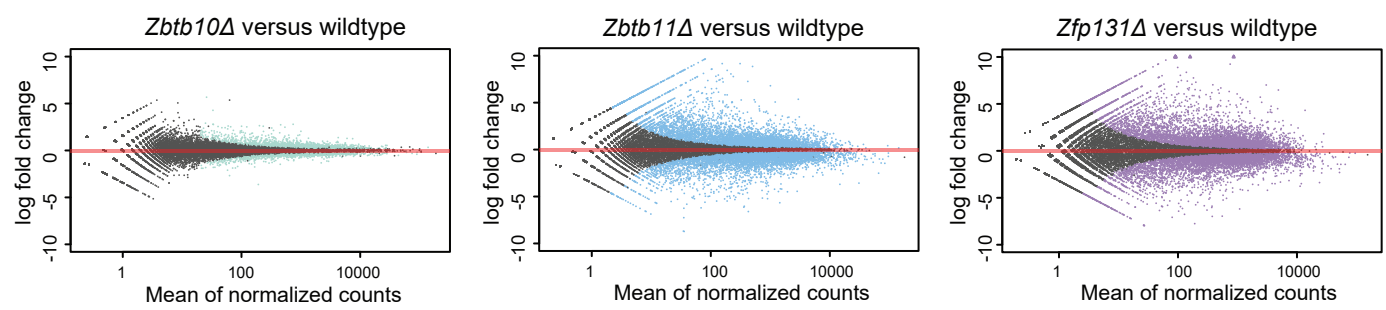
(A) Schematic overview of the cell-growth competition assay. Monoclonal mutant *Zbtb10* Δ , *Zbtb11* Δ , and *Zfp131* Δ cells compete with GFP-labeled wt ESCs.

(B) Percentage of non-GFP cells over time in cell growth competition assay of wt, *Zbtb10* Δ , *Zbtb11* Δ , and *Zfp131* Δ cells versus *H2b::Gfp* (n=3). Mirroring pooled mutant analysis, wt ESCs readily outcompete *Zbtb11* Δ and *Zfp131* Δ cells.

(C) OCT4/DAPI staining for wildtype, *Zbtb10* Δ , *Zbtb11* Δ and *Zfp131* Δ cells in 2i and LIF combination conditions (n=3). Statistical analysis was performed by student's t-test, *p<0.05, **p<0.005. *Zbtb11* Δ and *Zfp131* Δ cells have decreased OCT4 signal in specific culture conditions.

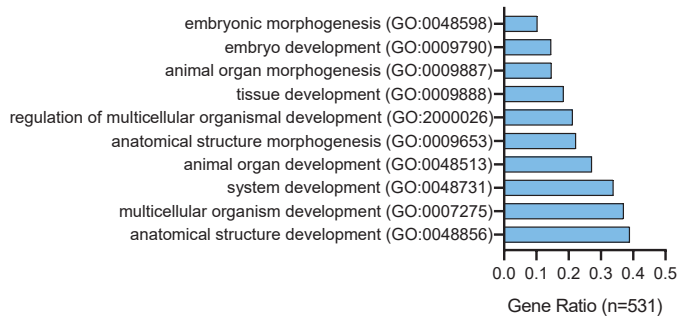
Figure S8

A



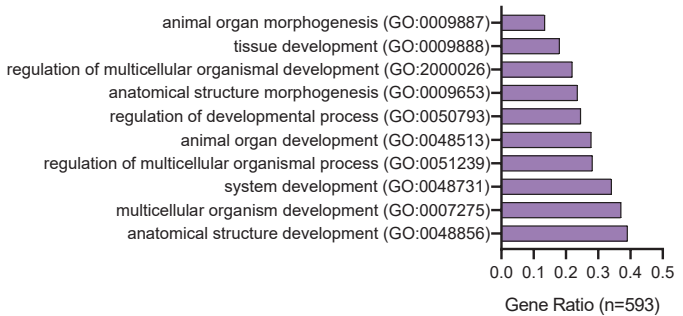
B

Significantly upregulated GO categories in *Zbtb11Δ* versus wildtype in +2i conditions



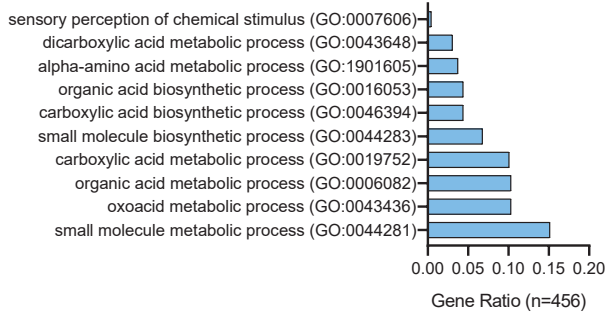
C

Significantly upregulated GO categories in *Zfp131Δ* versus wildtype in +2i conditions



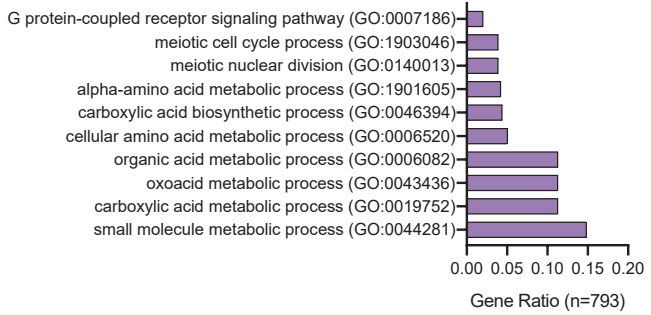
D

Significantly downregulated GO categories in *Zbtb11Δ* versus wildtype in +2i conditions



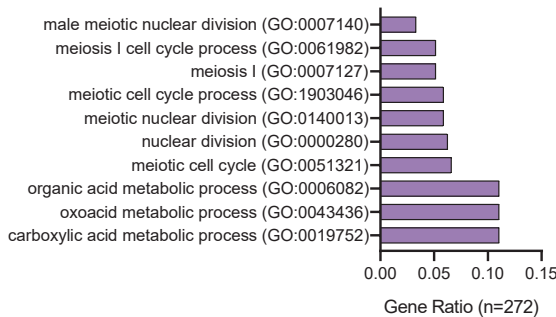
E

Significantly downregulated GO categories in *Zfp131Δ* versus wildtype in +2i conditions

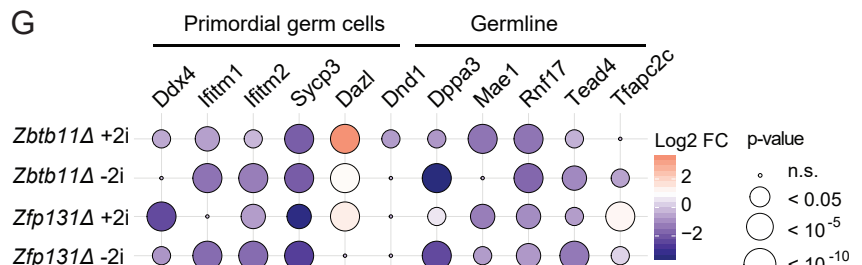


F

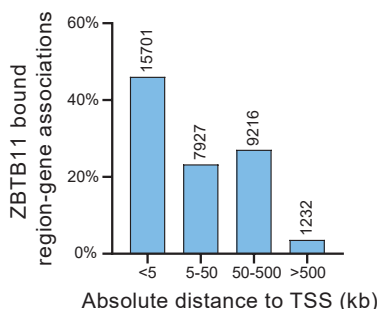
Significantly downregulated GO categories in *Zfp131Δ* versus wildtype in -2i conditions



G



H



I

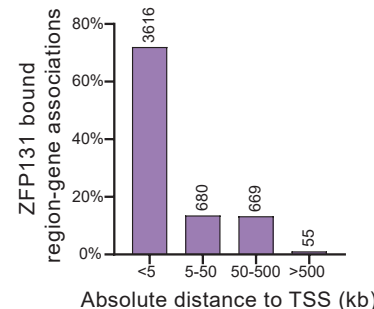


Figure S8. *Zbtb11* Δ and *Zfp131* Δ mutant cells express multiple lineage-specific markers in +2i conditions.

(A) Volcano plots of log2 fold change of transcripts expressed in *Zbtb10* Δ , *Zbtb11* Δ and *Zfp131* Δ cells versus wt cells grown in the absence of doxycycline for 3d in +2i+LIF media (n=2). Significant changes (* p<0.05) marked in color for each genotype. *Zbtb11* and *Zfp131* mutations induce aberrant gene expression.

(B) GO-enrichment analysis of significantly upregulated genes in *Zbtb11* Δ in +2i condition (n=531), **(C)** significantly upregulated genes in *Zfp131* Δ in +2i condition (n=593), **(D)** significantly downregulated genes in *Zbtb11* Δ in +2i condition (n=456), **(E)** significantly downregulated genes in *Zfp131* Δ in +2i condition (n=793), and **(F)** significantly downregulated genes in *Zfp131* Δ in -2i condition (n=272). Gene Ratio is calculated with the number of occurrences in specific GO categories divided by the total amount of genes. The low number of downregulated genes in -2i conditions for *Zbtb11* Δ produced no significant GO-term enriched.

(G) The log2 fold change of TFs obtained from bulk RNAseq experiment in *Zbtb11* Δ and *Zfp131* Δ cells versus wildtype in plus and minus 2i conditions. (n.s. Not significant, * < 0.05, ** < 10⁻⁵, *** < 10⁻¹⁰) (n=2). No aberrant expression of primordial germ cells and germline TFs detected in *Zbtb11* Δ and *Zfp131* Δ cells.

(H) The proximity of all ZBTB11 and **(I)** ZFP131 bound regions to TSS. Both TFs bind proximal to TSSs.

Figure S9

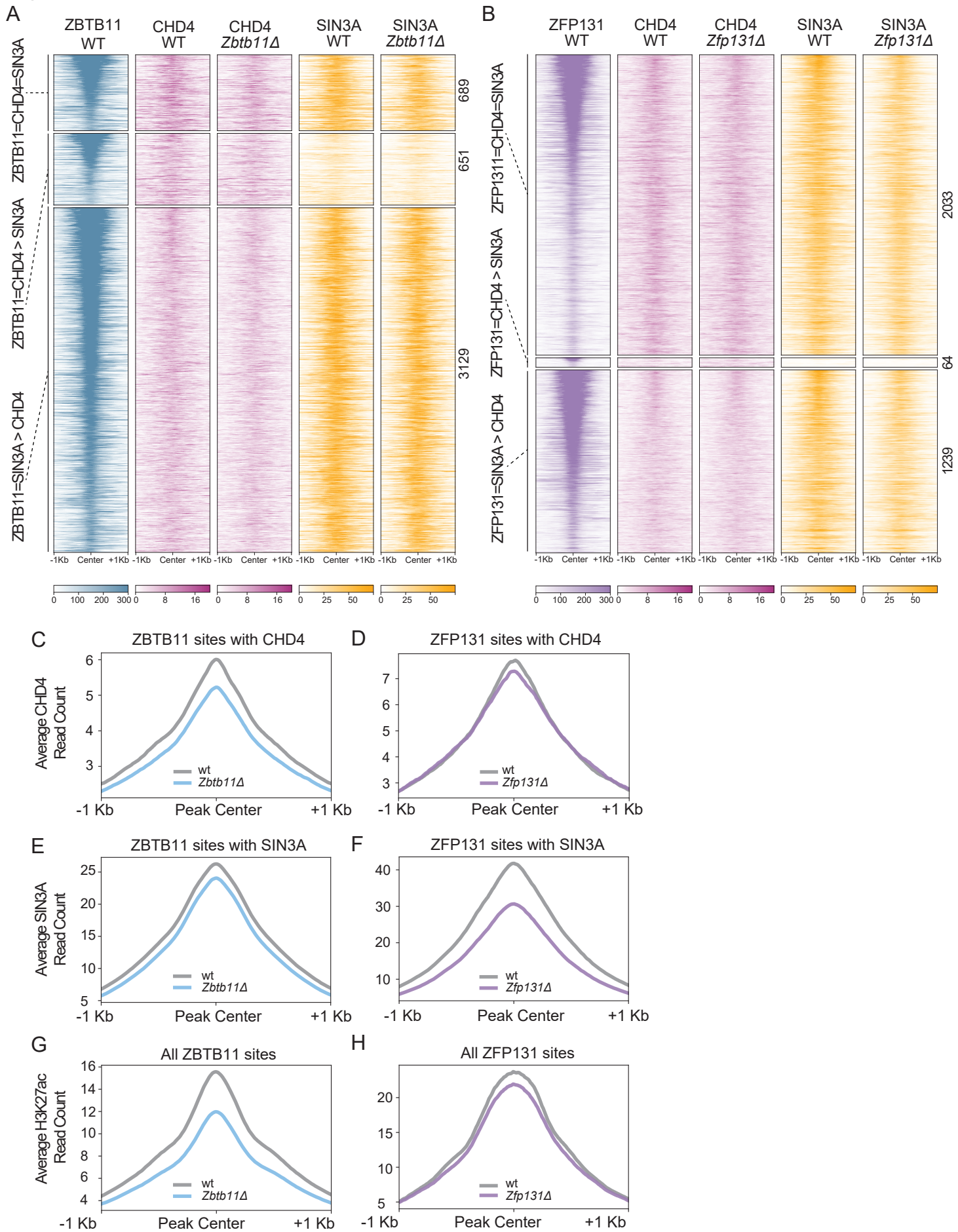


Figure S9. ZBTB11 and ZFP131 cobound with CHD4 and SIN3A.

- (A)** ChIP-seq heatmap for ZBTB11 overlap with CHD4 and SIN3A in *Zbtb11* Δ and wt cells (n=2 for all).
- (B)** ChIP-seq heatmap for ZFP131 overlap with CHD4 and SIN3A in *Zfp131* Δ and wt cells (n=2 for all).
- (C)** Metagene plots for CHD4 binding difference in *Zbtb11* Δ versus wt (n=2) and in **(D)** *Zfp131* Δ versus wt (n=2). Both mutants have a slight decrease in CHD4 binding in mutant vs wt.
- (E)** Metagene plots for SIN3A binding difference in *Zbtb11* Δ versus wt (n=2) and in **(F)** *Zfp131* Δ versus wt (n=2). Both mutants have a slight decrease in SIN3A binding in mutant vs wt.
- (G)** Metagene plots for H3K27ac at ZBTB11 bound sites in *Zbtb11* Δ and wt ESCs (n=2) and **(H)** at ZFP131 bound sites in *Zfp131* Δ versus wt (n=2). Both mutants have a decrease in H3K27ac contrary to the expected increase.